



Hyperinsulinemia Is Highly Associated With Markers of Hepatocytic Senescence in Two Independent Cohorts

Abraham S. Meijnikman,^{1,2} Casper C. van Olden,¹ Ömrüm Aydin,^{1,2} Hilde Herrema,¹ Dorota Kaminska,³ Dimitra Lappa,⁴ Ville Männistö,⁵ Valentina Tremaroli,⁶ Louise E. Olofsson,⁶ Maurits de Brauw,² Arnold van de Laar,² Joanne Verheij,⁷ Victor E.A. Gerdes,^{1,2} Thue W. Schwartz,⁸ Jens Nielsen,⁴ Fredrik Bäckhed,^{6,9,10} Päivi Pajukanta,^{11,12} Jussi Pihlajamäki,^{3,5} Tamar Tchkonja,¹³ James L. Kirkland,¹³ Folkert Kuipers,¹⁴ Max Nieuwdorp,¹ and Albert K. Groen^{1,14}

Diabetes 2022;71:1929–1936 | <https://doi.org/10.2337/db21-1076>

Cellular senescence is an essentially irreversible growth arrest that occurs in response to various cellular stressors and may contribute to development of type 2 diabetes mellitus and nonalcoholic fatty liver disease (NAFLD). In this article, we investigated whether chronically elevated insulin levels are associated with cellular senescence in the human liver. In 107 individuals undergoing bariatric surgery, hepatic senescence markers were assessed by immunohistochemistry as well as transcriptomics. A subset of 180 participants from the ongoing Finnish Kuopio Obesity Surgery (KOBS) study was used as validation cohort. We found plasma insulin to be highly associated with various markers of cellular senescence in liver tissue. The liver transcriptome of individuals with high insulin revealed significant upregulation of several genes associated with senescence: *p21*, *TGFβ*, *PI3K*, *HLA-G*, *IL8*, *p38*, *Ras*, and *E2F*. Insulin associated with hepatic senescence independently of NAFLD

and plasma glucose. By using transcriptomic data from the KOBS study, we could validate the association of insulin with *p21* in the liver. Our results support a potential role for hyperinsulinemia in induction of cellular senescence in the liver. These findings suggest possible benefits of lowering insulin levels in obese individuals with insulin resistance.

Cellular senescence is one of the hallmarks of aging (1). It is defined as a stable arrest of the cell cycle coupled to specific phenotypic changes (1). Senescent cells can secrete a collection of proteins and other factors, termed the senescence-associated secretory phenotype (SASP) (2,3). It is now generally accepted that cellular senescence contributes to aging phenotypes, and accumulating evidence shows that senescence is associated with age-related diseases, such as type 2 diabetes mellitus (T2DM)

¹Departments of Internal and Experimental Vascular Medicine, Amsterdam University Medical Centers, Location AMC, Amsterdam, the Netherlands

²Department of Surgery, Spaarne Hospital, Hoofddorp, the Netherlands

³Institute of Public Health and Clinical Nutrition, University of Eastern Finland, Kuopio, Finland

⁴Systems and Synthetic Biology, Department of Biology and Biological Engineering, Chalmers University of Technology, Gothenburg, Sweden

⁵Department of Medicine, Endocrinology and Clinical Nutrition, Kuopio University Hospital, Kuopio Finland

⁶Wallenberg Laboratory, Department of Molecular and Clinical Medicine, Sahlgrenska Academy, University of Gothenburg, Gothenburg, Sweden

⁷Department of Pathology, University Medical Centers, University of Amsterdam, Cancer Center Amsterdam, Amsterdam, the Netherlands

⁸Laboratory for Molecular Pharmacology, Department of Neuroscience and Pharmacology, Faculty of Health and Medical Sciences, University of Copenhagen, Copenhagen, Denmark

⁹Novo Nordisk Foundation Center for Basic Metabolic Research, Faculty of Health and Medical Sciences, University of Copenhagen, Copenhagen, Denmark

¹⁰Region Västra Götaland, Department of Clinical Physiology, Sahlgrenska University Hospital, Gothenburg, Sweden

¹¹Department of Human Genetics, David Geffen School of Medicine at UCLA, Los Angeles, CA

¹²Institute for Precision Health, David Geffen School of Medicine at UCLA, Los Angeles, CA

¹³Robert and Arlene Kogod Center on Aging, Mayo Clinic, Rochester, MN

¹⁴Departments of Pediatrics and Laboratory Medicine, University of Groningen, University Medical Center Groningen, Groningen, the Netherlands

Corresponding author: Albert K. Groen, a.k.groen@amsterdamumc.nl

Received 24 November 2021 and accepted 25 May 2022

This article contains supplementary material online at <https://doi.org/10.2337/figshare.20051795>.

A.S.M. and C.C.v.O. contributed equally to this work.

© 2022 by the American Diabetes Association. Readers may use this article as long as the work is properly cited, the use is educational and not for profit, and the work is not altered. More information is available at <https://www.diabetesjournals.org/journals/pages/license>.

and nonalcoholic fatty liver disease (NAFLD) (4–6). Although causality is yet to be established in humans, current evidence suggests that targeting of senescent cells has novel treatment potential for the treatment of several age-related diseases, including T2DM and NAFLD (7,8).

In search of mechanisms that drive cellular senescence, the focus has been on factors associated with insulin resistance, such as chronic inflammation and elevated glucose and lipid levels (9). Although studies investigating the role of insulin itself in the development of cellular senescence are scarce, a causal role in inducing cellular senescence in adipose tissue was recently established (10). Since hyperinsulinemia is one of the shared key features of aging, obesity, T2DM, and NAFLD (11–13), we hypothesized that chronically elevated insulin levels may be associated with cellular senescence in liver tissue in humans, independent of NAFLD.

In this study, we investigated the relationship between plasma insulin levels and markers of senescence in a cohort of obese patients scheduled for bariatric surgery. The main results were validated in an independent cohort.

RESEARCH DESIGN AND METHODS

Participants were recruited from our bariatric surgery cohort as previously described (14). In brief, 107 individuals underwent a complete metabolic workup prior to their bariatric surgery procedure between September 2016 and the end of 2018. Within 2 months before surgery, a 2 h mixed-meal test (MMT) was performed. The MMT consisted of two Nutridrink compact 125 mL (Nutricia), in total containing 23.3 g fat, 74.3 g carbohydrates, and 24.0 g protein. Blood samples were drawn at baseline and then 10, 20, 30, 60, 90, and 120 min after ingestion of Nutridrink. In a subset of 23 individuals, samples from both portal and peripheral venous blood were drawn on the day of surgery. All samples were stored at -80°C until further processing. The study was performed in accordance with the Declaration of Helsinki and approved by the local Ethics Committee (approval code NL55755.018.15). All participants provided written informed consent.

Diabetes Definitions

Normal glucose tolerance and prediabetes definitions were in accordance with the American Diabetes Association (ADA) criteria (15). T2DM was defined as individuals who fulfilled the ADA criteria for diabetes, were treated with glucose-lowering agents, and/or had a history of T2DM.

Liver Biopsies and Histology

Biopsies were taken from segment three or five of the liver. All biopsies were snap-frozen in liquid nitrogen and stored at -80°C . Paraffin-embedded histological sections were stained with hematoxylin-eosin and Sirius red and scored according to the Steatosis, Activity, and Fibrosis score (16) by the Dutch Liver Pathology Panel. NAFLD was categorized into NAFL when steatosis was present in

$>5\%$ of hepatocytes alone or with mild inflammation but without ballooning or nonalcoholic steatohepatitis (NASH) when steatosis was present in $>5\%$ of hepatocytes and if ballooning and inflammation were both present in the biopsy. p21, BCL-2, and p53 immunohistochemistry was performed on formalin-fixed sections using mouse anti-p21 (18–0401 clone EA10; Zymed), Dako/M0887 clone 124 subclass IgG1, and Thermo Fisher Scientific/Ms 738-P clone DO-7+BP53–12 subclass IgG2a/2b, respectively, both with secondary staining with BenchMark ULTRA (Ventana) as positive controls for p21 and p53 tonsil and p53-positive tumor with overexpression (Supplementary Fig. 1). Ten blinded, consecutive, nonoverlapping fields were acquired at $\times 400$ original magnification and counted manually.

Transcriptomics

RNA from the liver biopsies was extracted using the Tri-Pure Isolation Reagent (Roche). The extracted RNA was purified using RNeasy MinElute spin columns, and libraries for RNA sequencing were prepared using a ribosomal RNA depletion method and sequenced at Novogene. After ribosomal RNA depletion, the RNA was fragmented using fragmentation buffer. Double-stranded cDNA was then synthesized using mRNA template and random hexamer primers (for the first strand), followed by second-strand synthesis buffer, deoxynucleotide triphosphates, RNase H, and DNA polymerase I for the second strand. After a series of terminal repair, A ligation, and sequencing adaptor ligation, the cDNA library was size-selected and PCR-enriched. Library quality control was performed using Qubit 2.0 (library concentration), Agilent 2100 (insert size), and quantitative PCR (for precise effective library concentration).

Validation Cohort

A subset of 180 participants with liver mRNA sequencing data available from the ongoing Finnish Kuopio Obesity Surgery (KOBOS) study (17) was included in the validation cohort. All participants provided informed consent, and the study protocol was approved by the local ethics committee. Liver histology was evaluated by one experienced liver pathologist, and the study population was divided into those with normal liver, those with NAFLD, and those with NASH, as described above for the discovery cohort. RNA sequencing of strand-specific Ribo-Zero libraries was performed on the HiSeq 2500 (Illumina) with 50-bp paired-end reads. The reads mapped to exons (GRCh38 assembly, release 29) were counted with the Rsubread R package and normalized with the trimmed mean of M-values method using edgeR. Normalized read counts were converted to \log_2 -counts-per-million. Expression data were corrected for previously identified technical cofactors (18).

Statistics

Data are expressed as mean \pm SD for normally distributed variables or as median (interquartile range) when distributions were skewed. The normal distribution of continuous variables was assessed using the Kolmogorov-Smirnov method. To gain normality, variables with skewed distribution were log transformed. When the distribution was not normal, a Wilcoxon test was performed. For more than two groups, a Kruskal-Wallis test was performed. Correlation tests were performed using Pearson correlation coefficient, and P values were calculated using the t test when the distribution was normal and Spearman rank-order correlation and P values via the asymptotic t approximation when the distribution was not. Two-tailed significance was set at 0.05. Regression analyses were performed using multiple linear regression. For baseline variables, only participants with complete baseline variables were included. For missing data in the MMT, missing values were imputed using predictive mean matching using the MICE package (version 3.11.0). Transcriptomic data were analyzed using the following methods: abundances of transcripts were quantified using Kallisto. Counts were normalized and differential expression calculated using DESeq2. For analyses of senescence genes, subjects were stratified into two groups of quintiles. These groups were based on baseline insulin values. Differential expressions were calculated between the highest and lowest quintiles. Analysis of genes was limited to genes in the Kyoto Encyclopedia of Genes and Genomes (KEGG) senescence pathway. P values of differentially expressed genes were adjusted using the Benjamini and Hochberg method, and significance for false discovery was set at $P < 0.05$.

Data and Resource Availability

Data and resources used are available upon request.

RESULTS

The recruited participants were stratified based on glucose tolerance parameters according to ADA criteria (15). Thirty-five individuals had normal glucose tolerance, 48 had prediabetes, while 24 had T2DM. The clinical characteristics of the 107 individuals selected are summarized in Supplementary Table 1.

Liver biopsies of 56 patients were available for histological analysis. The robust senescence biomarker p21 (cyclin-dependent kinase inhibitor 1A) was used as a first screening marker: p21 protein levels were quantified by immunohistochemistry (Fig. 1A–C). Next, we quantified p53 to ensure robustness of the hepatocytic senescence signature (Fig. 1D–F). BCL-2 (antiapoptosis marker) was also quantified (Supplementary Fig. 2). To assess insulin resistance, we analyzed MMT data in which glucose, insulin, and triglycerides were measured at seven time points. Hepatic p21 expression correlated significantly with glucose area under the curve (AUC) ($r = 0.33$; $P = 0.009$), peripheral insulin ($r = 0.49$; $P < 0.001$), and insulin AUC ($r = 0.46$;

$P < 0.001$) during the MMT (Fig. 1G–I). In line with this, BCL-2 significantly correlated with glucose AUC ($r = 0.54$; $P = 0.033$), peripheral insulin ($r = 0.58$; $P = 0.018$), and insulin AUC ($r = 0.53$; $P = 0.036$) (Supplemental Fig. 3). For p53, a significant correlation was observed with peripheral insulin ($r = 0.52$; $P = 0.039$) (Supplementary Fig. 3). Fasting glucose did not correlate with BCL-2 or p53 expression.

Bearing in mind that the pancreas drains into the portal vein, highest concentrations of insulin are likely to be found in this blood compartment. In a subset of 23 individuals, we collected portal vein blood and observed a strong correlation between p21 expression and insulin levels in the portal vein ($r = 0.74$; $P < 0.001$) (Fig. 1J).

To further investigate the relationship between insulin and hepatocytic senescence, we performed RNA sequencing in liver biopsies derived from the 107 individuals. Transcriptomic analyses revealed differential expression in senescence-related genes between groups stratified for peripheral fasting insulin (Fig. 1K). The key cell cycle inhibitors *CDKN1A* (coding for p21) and *MAPK11* as well as genes encoding SASP factors, including *TGFBI* and *CXCL8*, were upregulated in the high insulin group. In addition, the transcription factors *E2F1* and *E2F3*, which control progression from the G₁ to S phase of the cell cycle (19), were higher in the high insulin group.

Next, we investigated if cellular senescence is associated with NAFLD. According to the Steatosis, Activity, and Fibrosis score, 22 individuals had no steatosis, 24 had NAFL, and 10 had NASH (Table 1). p21 protein expression was significantly higher in individuals with NASH compared with NAFL and individuals without steatosis (Fig. 2A). According to the MMT data, fasting insulin and insulin AUC increased with disease progression, substantiating that hepatic insulin resistance plays an important role in NAFLD pathogenesis (Fig. 2B and C). This is further demonstrated by the increased concentration of plasma triglycerides in individuals with NAFL and NASH (Fig. 2D), which may indicate a loss of suppression of apolipoprotein B expression by insulin and hence increased VLDL-triglyceride production (20). Interestingly, in patients with high portal vein insulin, increased expression of p21 was observed, suggesting that insulin is associated with senescence independent of NAFLD.

To further investigate interrelations among hyperinsulinemia, senescence, and NAFLD, we performed regression analysis. The regression model predicting p21 percentage, using either fasting peripheral insulin or the NAFLD classification, had an adjusted R^2 of 0.18, $F(1,58) = 14$, $P < 0.001$ and 0.39, $F(1,61) = 40$, $P < 0.001$, respectively. When using both insulin and NAFLD classification to predict p21 percentage, the adjusted R^2 was 0.45, $F(2,57) = 24.8$, $P < 0.001$, and both variables were significant predictors, indicating that insulin, independently from NAFLD, is associated with hepatocytic senescence. Neither fasting glucose nor glucose AUC were significant predictors when combined with fasting peripheral insulin and NAFLD.

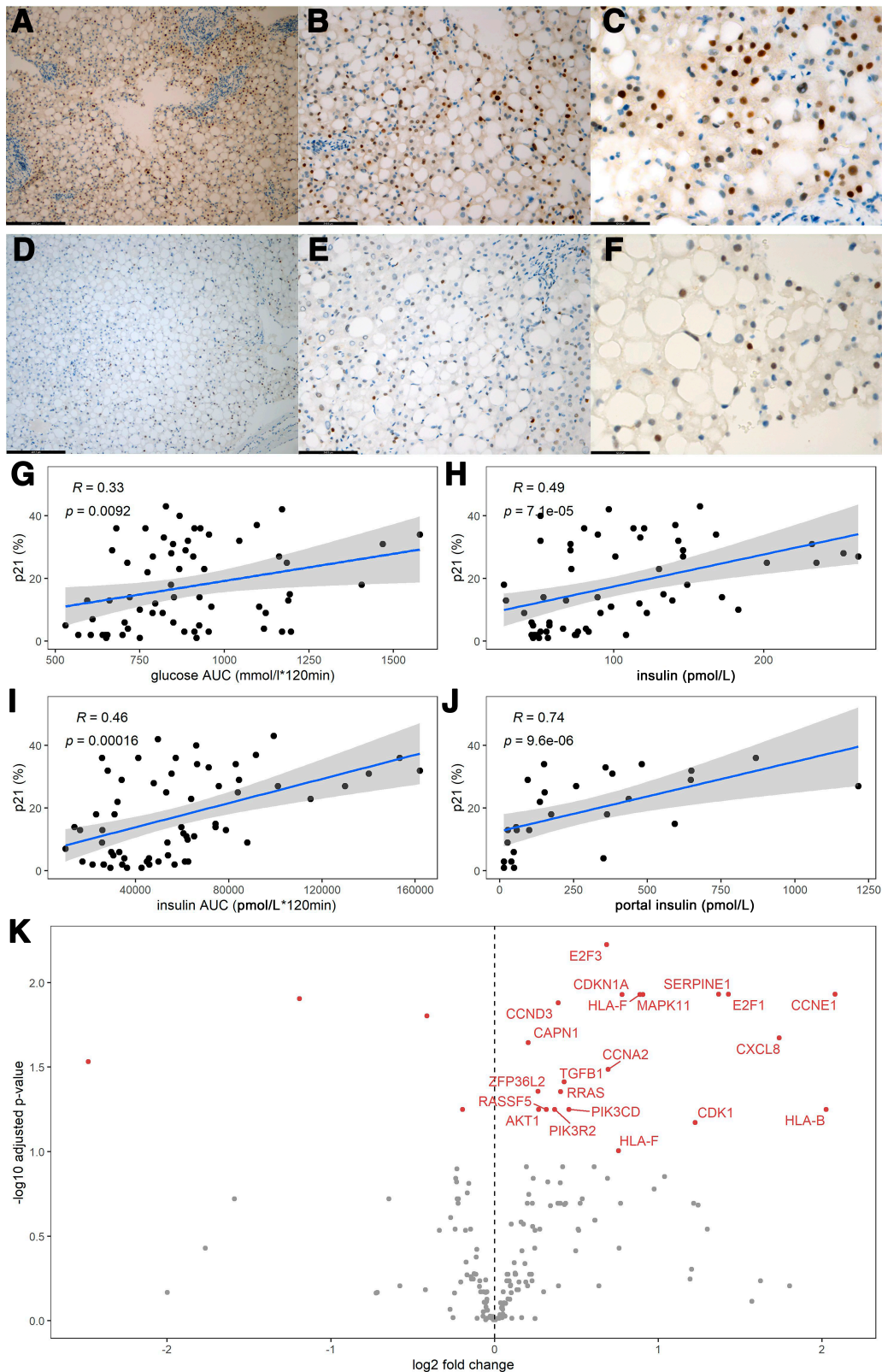


Figure 1—A–C: Representative images of immunohistochemistry staining of liver tissue with p21 with $\times 100$, $\times 200$, and $\times 400$ original magnification, respectively. D–F: Representative images of immunohistochemistry staining of liver tissue with p53 with $\times 100$, $\times 200$, and $\times 400$ original magnification, respectively. G–J: Scatterplots depicting the percentage of p21 on the y-axis and, respectively, glucose AUC, peripheral fasting insulin, insulin AUC, and portal insulin on the x-axis. The blue line is the linear regression prediction line, gray is the 95% CI of the regression, ρ is the Spearman correlation coefficient, and P value is the significance level. K: Volcano plot showing genes in the

Table 1—Comparison among individuals with no steatosis, NAFL, and NASH

Variables	No steatosis (n = 22)	NAFL (n = 24)	NASH (n = 10)
Sex (male/female)	3/19	10/14	2/8
Age (years)	43 (34–47)	49 (44–53)	51 (46–56)
BMI (kg/m ²)	39 (37–43)	40 (37–42)	40 (39–43)
T2DM (%)	1 (5)	5 (21)	3 (30)
Alkaline phosphatase (30–135 units/L)	88 (78–100)	79 (65–101)	72 (66–80)
γ-GT (10–40 IU/L)	22 (18–26)	32 (24–48)	19 (16–37)
ALT (0–50 IU/L)	24 (19–31)	38 (25–50)	33 (24–49)
AST (0–35 IU/L)	23 (20–26)	26 (22–30)	28 (26–34)
Ferritin (24–336 μg/L)	99 (37–130)	144 (61–215)	126 (82–192)
FPG (<5.6 mmol/L)	5.3 (5.0–5.5)	5.6 (5.1–6.6)	5.8 (5.6–6.7)
HbA _{1c} (<5.6%)	5.7 (5.4–5.8)	5.8 (5.4–6.0)	6.0 (5.7–6.4)
HbA _{1c} (mmol/mol)	39 (36–40)	40 (40–42)	42 (39–46.4)
Fasting insulin (18–48 pmol/L)	62 (48–81)	113 (71–141)	108 (82–155)
Total cholesterol (1.5–6.5 mmol/L)	4.7 (4.0–5.8)	4.8 (4.0–5.6)	5.1 (4.3–5.2)
Triglycerides (<1.7 mmol/L)	1.0 (0.8–1.4)	1.2 (1.0–1.7)	1.2 (1.0–1.3)

Data are expressed as median (interquartile range) and parentheses after variable name and depict units and, if applicable, reference values. FPG, fasting plasma glucose; γ-GT, γ-glutamyl transferase.

Adding insulin AUC to the model with NAFLD and fasting peripheral insulin did not improve the R^2 or the Akaike information criterion.

To validate our findings, we analyzed data from 180 individuals from an independent cohort from whom clinical data, liver histology, and liver transcriptomics data were available (Supplementary Table 2). In line with outcomes from our study, hepatic *CDKN1A* (*p21*) expression correlated with insulin resistance and NAFLD in the KOBS study ($r = 0.38$; $P < 0.001$) (Fig. 3). Moreover, stratifying individuals from the validation cohort by insulin levels revealed a strong cellular senescence signature, nine genes in the KEGG senescence pathway showed increased expression (Fig. 3E). In addition, we used the same regression model and found that insulin was associated with hepatocytic senescence independently of NAFLD. Predicting *CDKN1A* using fasting peripheral insulin and NAFL classification had an adjusted R^2 of 0.10, $F(1,115) = 14$ ($P < 0.001$) and 0.18, $F(1,119) = 28$ ($P < 0.001$), respectively. The combined model had an adjusted R^2 of 0.22, $F(2,114) = 17$ ($P < 0.001$), with both variables being significant predictors, validating the findings in our other cohort.

DISCUSSION

The major finding of this study is the strong association between plasma insulin and the presence of senescence

markers in liver tissue derived from individuals undergoing bariatric surgery, suggesting that insulin might play a role in the induction of senescence.

Cellular senescence has been implicated in the development of T2DM and NAFLD (21). It has long been considered to be a consequence and not the cause of hepatic steatosis. However, studies in mice revealed a causal role for cellular senescence in development of hepatic steatosis (7,8). Removal of the senescent cells induced attenuation of hepatic lipid accumulation. Indeed, our data show a clear association between plasma insulin levels and hepatic steatosis (Fig. 2B and C). Furthermore, our data also indicate the possibility that the role of insulin may be more complex than just its role in controlling lipid accumulation. Protein expression of the senescence markers p21, p53, and BCL-2 in the liver increased with plasma insulin concentration. Moreover, at the transcriptional level, expression of the cell cycle regulators *CDKN1A* and *MAPK11* as well as multiple genes encoding SASP proteins were enhanced in individuals with high plasma insulin levels. Interestingly, multiple regression analysis showed that insulin correlated with senescence independently from NAFLD, indicating that insulin-induced senescence indeed may precede NAFLD. In line with this hypothesis, we noted that individuals without NAFLD with a relatively high expression of p21 also had high concentrations of insulin in their portal blood. Although our results are associative, we speculate that insulin rather than glucose

KEGG senescence pathway identified by RNA sequencing of liver tissue biopsies, respectively; red genes are those that are significantly upregulated in patients with the highest quintile peripheral insulin. RNA-sequencing data were adjusted for age, and individuals with T2DM were excluded from this analysis.

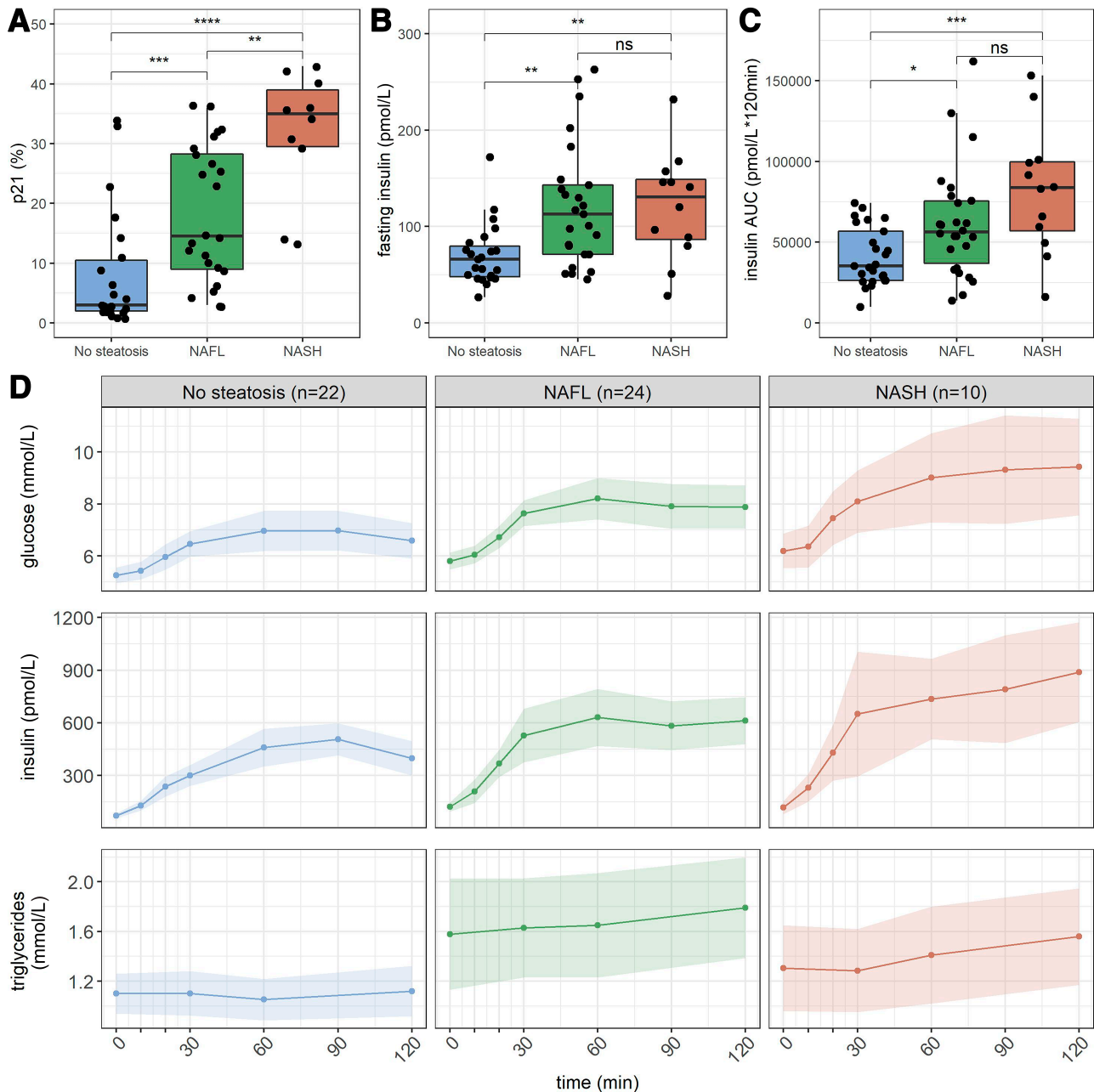


Figure 2—A–C: Box plots showing p21 percentage, peripheral fasting insulin, and insulin AUC on the y-axis and the different categories of NAFL displayed on the x-axis ($n = 56$). D: Glucose, insulin, and triglyceride excursions during a 2-h MMT comparing individuals with no steatosis, NAFL, and NASH. Data are means \pm 95% CIs. * $P < 0.05$, ** $P < 0.01$, *** $P < 0.001$.

might be an important factor for inducing cellular senescence in hepatocytes. To validate our results, we performed similar regression analyses in 180 individuals from the ongoing KOBS study (17). In line with data from our study, hepatic *CDKN1A* (p21) expression correlated with insulin resistance and NAFLD in the KOBS study ($r = 0.38$; $P < 0.001$). Also in this data set, multiple regression analysis revealed that insulin correlated independently from NAFLD and glucose with hepatic senescence markers. This suggests the possibility that hyperinsulinemia contributes to

senescence in the pathogenesis of NAFLD, at least partly, and insulin-induced senescence is upstream in the pathogenesis of NAFLD. This is in line with current evidence showing that insulin resistance precedes NAFLD (22). Also, our studies are in line with a recent article showing that insulin induces senescence in adipose tissue (10).

Limitations

We note that the analyses of human data sets in our study have some limitations. In this study, we used liver

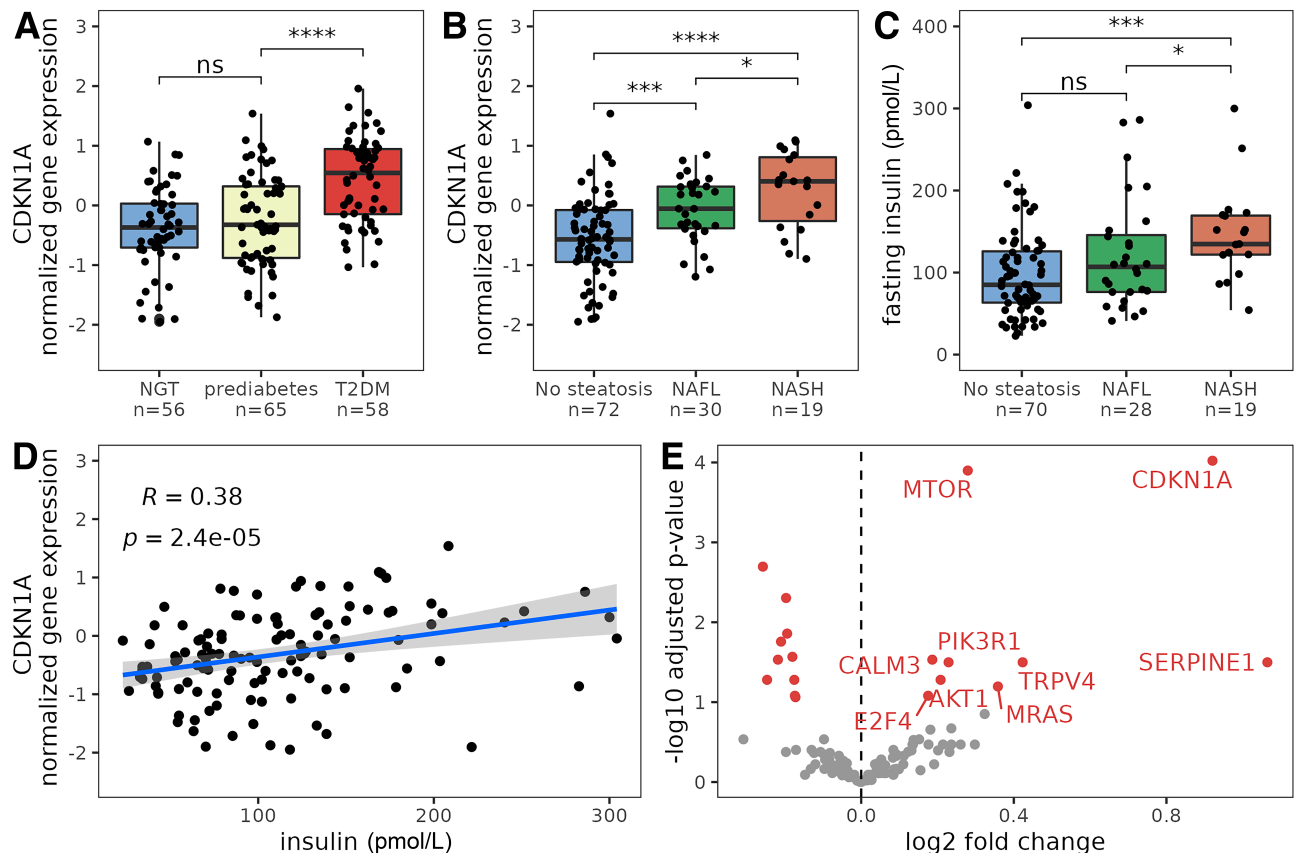


Figure 3—Results from the validation cohort ($n = 180$). **A:** Hepatic CDKN1A expression in individuals with normal glucose tolerance (NGT), impaired fasting glucose, or T2DM. **B:** Box plot of hepatic CDKN1A expression in individuals with no steatosis, NAFL, and NASH. **C:** Peripheral fasting insulin concentrations in individuals without NAFL and with NAFL and NASH; individuals with T2DM were excluded from this analysis. **D:** Scatterplot displaying the relation between peripheral insulin and CDKN1A expression. Blue line is the linear prediction regression line; gray area is 95% CI, ρ is Spearman correlation coefficient, and P is the significance level; individuals with T2DM were excluded from this analysis. **E:** Volcano plot showing genes in the KEGG senescence pathway identified by RNA sequencing of liver biopsies. Genes in red indicate that the gene is significantly upregulated in individuals with fasting insulin levels in the highest quintile group. Adjusted for age; individuals with T2DM were excluded from this analysis. * $P < 0.05$, ** $P < 0.01$, *** $P < 0.001$.

and plasma samples obtained from individuals who underwent bariatric surgery, which may introduce bias due to preoperative weight loss. However, individuals who had lost $>3\%$ of their body weight in the month prior to surgery or $>5\%$ during the 6 months before surgery were excluded. Last, we used transcriptomics data to validate our findings. To what extent the senescence markers signature found in the transcriptomics data reflect a “true” senescent signature remains to be answered.

In summary, we have shown by using two independent cohorts that plasma insulin levels correlate with markers of cellular senescence in liver tissue. Further studies are needed to investigate to what extent insulin is causally involved in inducing senescence in the liver.

Acknowledgments. The authors thank the nursing staff and all participating individuals for making this study possible and Manuela Krämer and Robert Jakubowicz (Wallenberg Laboratory, University of Gothenburg) for the preparation of the samples. The authors also thank the CSC-IT Center for

Science, Finland, for computational resources and pathologist Vesa Kärjä for histological characterization in KOBS cohort (Department of Pathology, University of Eastern Finland) and the members of the Dutch Liver Pathology Panel: Carolien M. Bronkhorst (Jeroen Bosch Hospital), Michael Doukas (Erasmus MC), Paul Drillenburg (OLVG Amsterdam), Arantza Farina (Amsterdam University Medical Centers), Natascha N.T. Goemaere (Maasstad Hospital), Mieke Jonker (Gelre Hospitals), Miangela M. Lacle (University Medical Center Utrecht), and Iryna Samarski (Maastricht UMC).

Funding. This study was funded by Leducq consortium grant CVD01 and the Novo Nordisk Foundation (NNF150C0016798). D.K. was supported by Academy of Finland grant (contract 316458). The KOBS study (principal investigator J.P.) was supported by Kuopio University Hospital Project grants (EVO/VTR grants 2005–2019) and an Academy of Finland grant (contract no. 138,006). A.S.M. is supported by EFS/Lilly. F.K. is supported by the Noaber Foundation. T.T. and J.L.K. were supported by National Institutes of Health grants AG013925 and AG062413 and the Translational Geroscience Network (AG061456), Robert and Arlene Kogod Center on Aging, the Connor Group, Robert J. and Theresa W. Ryan, and the Ted Nash Long Life and Noaber Foundations.

Duality of Interest. M.N. is on the Scientific Advisory Board of Caelus Health, Amsterdam, the Netherlands. F.B. is on the board of directors of Me-tabogen AB, Sweden. However, none of these possible conflicts of interest

bear direct relation to the outcomes of this specific study. T.T. and J.L.K. have a financial interest related to this research: patents on senolytic drugs and their uses are held by Mayo Clinic. This research has been reviewed by the Mayo Clinic Conflict of Interest Review Board and was conducted in compliance with Mayo Clinic Conflict of Interest policies. No other potential conflicts of interest were reported.

Author Contributions. A.S.M., C.C.v.O., O.A., M.d.B., and A.v.d.L. performed the patient visits and were involved in the recruitment of individuals. A.S.M. and C.C.v.O. performed the data analyses. H.H. and V.T. were responsible for sample processing. D.K. analyzed the RNA-sequencing data and performed the statistical analyses of the KOBS validation cohort. V.M. was responsible for the clinical data and interpretation of the KOBS. J.P. is the principal investigator of the KOBS cohort. V.E.A.G., T.T., J.L.K., F.K., M.N., and A.K.G. designed the study and supervised all parts of the project. A.S.M., C.C.v.O., H.H., and A.K.G. drafted the manuscript. All authors provided support and constructive criticism throughout the project and approved the final version of the article. A.G. is the guarantor of this work and, as such, had full access to all of the data in the study and takes responsibility for the integrity of the data and the accuracy of the data analysis.

References

- López-Otín C, Blasco MA, Partridge L, Serrano M, Kroemer G. The hallmarks of aging. *2013*;153:1194–1217
- Ogrodnik M, Salmonowicz H, Gladyshev VN. Integrating cellular senescence with the concept of damage accumulation in aging: relevance for clearance of senescent cells. *Aging Cell* 2019;18:e12841
- Minamino T, Orimo M, Shimizu I, et al. A crucial role for adipose tissue p53 in the regulation of insulin resistance. *Nat Med* 2009;15:1082–1087
- Palmer AK, Xu M, Zhu Y, et al. Targeting senescent cells alleviates obesity-induced metabolic dysfunction. *Aging Cell* 2019;18:e12950
- Gustafson B, Nerstedt A, Smith U. Reduced subcutaneous adipogenesis in human hypertrophic obesity is linked to senescent precursor cells. *Nat Commun* 2019;10:2757
- Aravinthan A, Scarpini C, Tachtatzis P, et al. Hepatocyte senescence predicts progression in non-alcohol-related fatty liver disease. *J Hepatol* 2013;58:549–556
- Meijnikman AS, Herrema H, Scheithauer TPM, Kroon J, Nieuwdorp M, Groen AK. Evaluating causality of cellular senescence in non-alcoholic fatty liver disease. *JHEP Rep* 2021;3:100301
- Ogrodnik M, Miwa S, Tchkonja T, et al. Cellular senescence drives age-dependent hepatic steatosis. *Nat Commun* 2017;8:15691
- Palmer AK, Gustafson B, Kirkland JL, Smith U. Cellular senescence: at the nexus between ageing and diabetes. *Diabetologia* 2019;62:1835–1841
- Li Q, Hagberg CE, Silva Cascales H, et al. Obesity and hyperinsulinemia drive adipocytes to activate a cell cycle program and senesce. *Nat Med* 2021;27:1941–1953
- Gumbiner B, Polonsky KS, Beltz WF, Wallace P, Brechtel G, Fink RI. Effects of aging on insulin secretion. *Diabetes* 1989;38:1549–1556
- Arab JP, Arrese M, Trauner M. Recent Insights into the Pathogenesis of Nonalcoholic Fatty Liver Disease. *Annu Rev Pathol* 2018;13:321–350
- Corkey BE. Banting lecture 2011: hyperinsulinemia: cause or consequence? *Diabetes* 2012;61:4–13
- Van Olden CC, Van de Laar AW, Meijnikman AS, et al. A systems biology approach to understand gut microbiota and host metabolism in morbid obesity: design of the BARIA Longitudinal Cohort Study. *J Intern Med* 2021;289:340–354
- American Diabetes Association. 2. Classification and diagnosis of diabetes: *Standards of Medical Care in Diabetes—2020*. *Diabetes Care* 2020; 43(Suppl. 1):S14–S31
- Bedossa P; FLIP Pathology Consortium. Utility and appropriateness of the fatty liver inhibition of progression (FLIP) algorithm and steatosis, activity, and fibrosis (SAF) score in the evaluation of biopsies of nonalcoholic fatty liver disease. *Hepatology* 2014;60:565–575
- Simonen M, Männistö V, Leppänen J, et al. Desmosterol in human nonalcoholic steatohepatitis. *Hepatology* 2013;58:976–982
- Männistö V, Kaminska D, Käkälä P, et al. Protein phosphatase 1 regulatory subunit 3B genotype at rs4240624 has a major effect on gallbladder bile composition. *Hepatol Commun* 2020;5:244–257
- Rubin SM, Gall AL, Zheng N, Pavletich NP. Structure of the Rb C-terminal domain bound to E2F1-DP1: a mechanism for phosphorylation-induced E2F release. *Cell* 2005;123:1093–1106
- Wiegman CH, Bandsma RHJ, Ouwens M, et al. Hepatic VLDL production in ob/ob mice is not stimulated by massive de novo lipogenesis but is less sensitive to the suppressive effects of insulin. *Diabetes* 2003;52:1081–1089
- Papatheodoridi A-M, Chrysavgis L, Koutsilieris M, Chatzigeorgiou A. The role of senescence in the development of non-alcoholic fatty liver disease and progression to non-alcoholic steatohepatitis. *Hepatology* 2020;71:363–374
- Khan RS, Bril F, Cusi K, Newsome PN. Modulation of insulin resistance in nonalcoholic fatty liver disease. *Hepatology* 2019;70:711–724